INL/JOU-23-74074-Revision-0

Low temperature hydrogen superpermeation in vanadium composite metal foil pumps

December 2023

Changing the World's Energy Future

Chao Li, Thomas F Fuerst, J. Douglas Way, Colin Wolden

INL/JOU-23-74074-Revision-0

Low temperature hydrogen superpermeation in vanadium composite metal foil pumps

Chao Li, Thomas F Fuerst, J. Douglas Way, Colin Wolden

December 2023

Idaho National Laboratory
Idaho Falls, Idaho 83415

http://www.inl.gov

Prepared for the
U.S. Department of Energy
Under DOE Idaho Operations Office
Contract DE-AC07-05ID14517

Nuclear Materials and Energy 37 (2023) 101529

Contents lists available at ScienceDirect

Nuclear Materials and Energy

journal homepage: www.elsevier.com/locate/nme

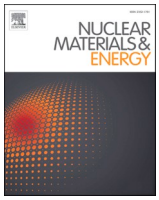

Low temperature hydrogen superpermeation in vanadium composite metal foil pumps

Chao Li [a], J. Douglas Way [a], Thomas F. Fuerst [b], Colin A. Wolden [a,*]

[a] Department of Chemical & Biological Engineering, Colorado School of Mines, Golden, CO 80401, United States
[b] Fusion Safety Program, Idaho National Laboratory, Idaho Falls, ID 83415, United States

ARTICLE INFO

Keywords:
Vanadium
Superpermeation
Hydrogen
Metal foil pump
Fusion fuel cycle

ABSTRACT

Palladium-based foil membranes are an effective option for hydrogen isotope recovery from the plasma exhaust of future fusion plants, but cost and availability are concerns. Vanadium (V) is a relatively low cost, neutron tolerant material with high hydrogen permeability. It has been well-studied as a superpermeable membrane at high temperature (>500 °C), but V displays negligible superpermeation at low temperature (75–200 °C) due to catalytic limitations. Composite membranes were fabricated by depositing thin layers (~100 nm) of either Pd or BCC PdCu on sputter-cleaned vanadium foils (100 μm). Symmetric membranes elevated superpermeation to levels approaching bulk Pd or PdCu foils, with ~5X higher flux in the latter reflecting the superior properties of PdCu. Asymmetric membranes revealed that the Pd-based catalyst layer was critical for both efficient absorption of superthermal hydrogen upstream as well as catalyzing re-combinative desorption downstream. At T ≥ 150 °C composite membrane superpermeation was equivalent to the Pd-based foils, but the flux was attenuated by a factor of 2-3X as the temperature was reduced. This deviation from pure foil performance coincided with the formation of vanadium hydride (β-V_2H), which also impacted the transient response. Nevertheless, no embrittlement was observed under the conditions examined and elevating the temperature >150 °C removed the hydride and restored full performance. The achievement of palladium-level performance with a >99% reduction in Pd inventory makes these V composite metal foils pumps an attractive option for low temperature hydrogen isotope recovery in future fusion plants.

1. Introduction

Last year scientists at the US National Ignition Facility (NIF) demonstrated a laser-driven fusion reaction that marked the first time that more energy was produced from controlled fusion than was supplied [1]. Earlier this year United States Department of Energy announced its first awards in concert with its decadal vision for fusion commercialization [2,3]. Moreover, this public investment is dwarfed by the nearly $5 billion in private investment recently secured by fusion companies [4]. Thus, after decades of advances in plasma physics, an inflection point has been reached in the road to commercial fusion power generation where controlled fusion is no longer "always 30 years away" as the famous quip puts it [5]. However, as companies innovate confinement concepts for enabling Q > 1 plasma fusion, it is pertinent to acknowledge that the realization of fusion as a viable and practical energy source necessitates the successful resolution of various technical and engineering challenges to enable sustainable and safe power plant operation.

Notably, safe and efficient fuel management emerges as a prominent hurdle in this endeavor [6,7]. Currently, the leading concepts revolve around the fusion of hydrogen isotopes, specifically deuterium (D) and tritium (T), resulting in the production of helium and the release of a high-energy neutron [8]. While deuterium is relatively plentiful in supply as a fuel source, the utilization of tritium faces challenges due to its radioactivity and short half-life, requiring on-site generation and recycling [9]. In addition, in fusion plasma only a fraction of D/T undergoes conversion to helium, leading to the need for efficient purification and recovery methods [10]. A straightforward design entails the construction of a separate tritium plant [11], which demands substantial on-site tritium inventories, resulting in cost implications and safety concerns. Direct internal recycling (DIR) [12,13] is a promising alternative aimed at recovering unburnt fuel from the plasma exhaust in fusion systems. By directly reintroducing the isotopes back into the fueling system, DIR reduces the size requirements of tritium plants and

* Corresponding author.
E-mail address: cwolden@mines.edu (C.A. Wolden).

https://doi.org/10.1016/j.nme.2023.101529
Received 7 August 2023; Received in revised form 20 September 2023; Accepted 27 September 2023
Available online 28 September 2023

the necessary tritium inventory. The key technology enabling DIR is the metal foil pump (MFP) [14,15], a metallic membrane that selectively permeates hydrogen isotopes while preventing the passage of helium and impurities.

In a DIR design the MFPs can be deployed either near the divertor region, exposing it to superthermal hydrogen isotopes but risking rapid degradation from energetic neutrons, ion bombardment, and extreme temperatures, or farther downstream in the pump train, mitigating neutron and temperature exposure but necessitating a secondary source for superthermal hydrogen generation [16–18]. In both scenarios, it is anticipated that MFPs will function within a pressure range that can be tailored to match the divertor conditions, with an expectation of being ~10 Pa [19], which limits the efficacy of conventional pressure driven permeation due to the low driving force. MFPs operate through the principle of superpermeation [20–22]. In this process superthermal hydrogen atoms/ions, produced by plasma or thermal sources, can directly enter the metal bulk [22,23]. This results in bulk hydrogen concentration surpassing thermal equilibrium and a hydrogen flux that significantly exceeds conventional pressure-driven permeation. In these metals hydrogen diffusion is sufficiently fast that the concentration throughout the membrane is nominally uniform. Vacuum is applied to the downstream and hydrogen isotopes undergo re-combinative desorption. The unilateral transport due to implantation of hydrogen on the plasma-facing surface yields an effective pumping capacity with a selectivity exclusive to hydrogen isotopes, hence the name Metal Foil Pump.

The majority of superpermeation and MFP research has focused on pure metals, especially Group 5 metals such as V and Nb [24–29]. These studies primarily investigated MFP operation at high temperature (>500 °C) under high vacuum conditions characterized by relatively low incident flux. The main objective of these studies is to understand the underlying mechanisms, particularly addressing the influence of surface impurity layers and plasma properties. Operating at high temperatures effectively alleviates complications associated with hydrogen embrittlement, which can be problematic for Group 5 metals. Furthermore, other materials such as Fe [30], Ni [31] and Cu [32] have also been reported for hydrogen superpermeability studies, demonstrating their potential in this field. Comprehensive models [22,23,33] have been developed to capture and explain the observed behavior of pure metals operating under high temperature and low atomic hydrogen incident flux conditions.

In the low-temperature regime (<250 °C) most studies have focused on Pd due to its high catalytic activity and resistance to embrittlement. Early investigations were typically conducted under conditions of relatively low incident flux, with the primary objectives being to comprehend the impact of surface impurities on superpermeation and to quantify hydrogen recombination kinetics on Pd surfaces [34–37]. More recently, Takagi and co-workers conducted research on Pd [38] and PdCu [39] using deuterium plasma, with a dual focus on developing diagnostics for the QUEST reactor and gaining insights into asymmetric surface kinetics. The hydrogen permeation flux under these conditions can be calculated using **Eq. (1)** [38,39], which is dependent on the downstream desorption coefficient k_d ($m^4 \bullet s^{-1}$) and the bulk hydrogen concentration $[H]$ (m^{-3}):

$$J_H = k_d[H]^2 \tag{1}$$

In a recent study [40], we systematically investigated hydrogen superpermeation through foils of Pd and its alloys, PdAg and PdCu, under a combination of low temperature (60–200 °C) and high incident flux conditions. With appropriate surface cleaning we achieved atomic hydrogen fluxes exceeding 10^{-2} mol(H)·m^{-2}·s^{-1}, more than order of magnitude greater than previously obtained with Pd, and even greater than the best high temperature results with BCC foils [13,24,26]. The performance was consistent with **Eq. (1)**, with flux increasing as the temperature was reduced showing that absorption superthermal hydrogen was the primary rate-limiting step. Among these foils the best results were achieved with PdCu due to its superior recombinative desorption kinetics.

Composite membranes offer the potential to decouple surface and bulk properties and to independently tailor surfaces to enhance absorption upstream and desorption downstream. A common approach to create asymmetry is through the intentional introduction of contaminants (e.g. C, O, S containing moieties) to the feed surface [41–47]. The concept, exploited extensively in high temperature studies of BCC metals, was to form an impurity monolayer that did not inhibit absorption of superthermal hydrogen but prevented desorption of molecular hydrogen upstream. Less studied has been composite membranes consisting of multiple materials. In an early study by Shmayda et al. [48] examined copper-AISI 1008 steel composites. In this two-layer system orientation mattered, with superpermeation only observed with the Cu facing upstream, and barely any permeation when the sample was reversed with Cu facing downstream. Likewise, Andrew and Haase [49] showed in Pd|Cu composites that the Cu layer needs to be on the feed side in order to achieve an enhanced flux compared to pure Pd membranes. Additionally, they noted that the thickness of the Cu layer is significant. Coatings with a thickness of 3–5 nm exhibited enhancement in permeation flux, while thicker coatings (>13 nm) reduced the permeation flux. The same authors studied iron foil based composites (Pd|Fe, Pd|Fe|Cu) [50], and the highest flux was observed in the Pd|Fe|Cu composite with the Cu layer oriented to face the incident H atoms. More recently, Xu et al. [51] reported that applying a 1 μm sputter-deposited tungsten coating on F82H (feed-side) significantly increased deuterium plasma-driven permeation flux by about two orders of magnitude at 250 °C. This enhancement was attributed to much higher isotope solubility in the coating, which also led to a significant prolongation of the breakthrough time. In these studies, both the incident and permeated flux was very low, but they highlight both the potential and shortcomings of composite membranes. With appropriate orientation composite metal foil pumps can exceed the performance of the base metal foils. However, the introduction of additional interfaces can also create barriers that impede transport.

Despite the high flux achieved in our work with Pd-based foils, the cost and availability of Pd remains a concern. The goal of this work was to retain this performance while dramatically reducing the Pd inventory through the use of composite membranes. In this work, we explore the Pd or PdCu coated V composites for hydrogen superpermeation at low temperature (75–200 °C). With the exception of studies of impurity introduction [43,46,47] there are no reports of V-based engineered composite MFPs. Vanadium is an attractive base metal since it has much higher permeability than either Pd or PdCu and its hydrogen diffusivity is nearly as great as PdCu in this temperature regime (**SI-**Fig. 1**)**. Additionally, vanadium and related alloys uniquely exhibits low levels of induced radioactivity when subjected to neutron irradiation [52,53], making it a desirable material for use in fusion environments where materials will be irradiated. Previous studies of superpermeation in V foils has been limited to T > 500° [43,46,47], due to its inability to absorb or desorb at hydrogen at low temperatures. At elevated temperature Pd-V interdiffusion can be a major concern [54], but this is insignificant below 300 °C [55]. Therefore, our investigation aims to explore V-based composite MFPs that combine the excellent bulk properties of V with the desirable surface properties of Pd or PdCu.

2. Experimental

2.1. Materials

In this study, cold-rolled V foils were used (99.8% purity, 100 μm thickness, ESPI materials, Ashland, OR, USA). Prior to conducting plasma permeation testing or materials deposition, an argon plasma cleaning process was carried out in an AJA sputtering chamber to remove impurities from the surface. The V-foil was clamped onto a

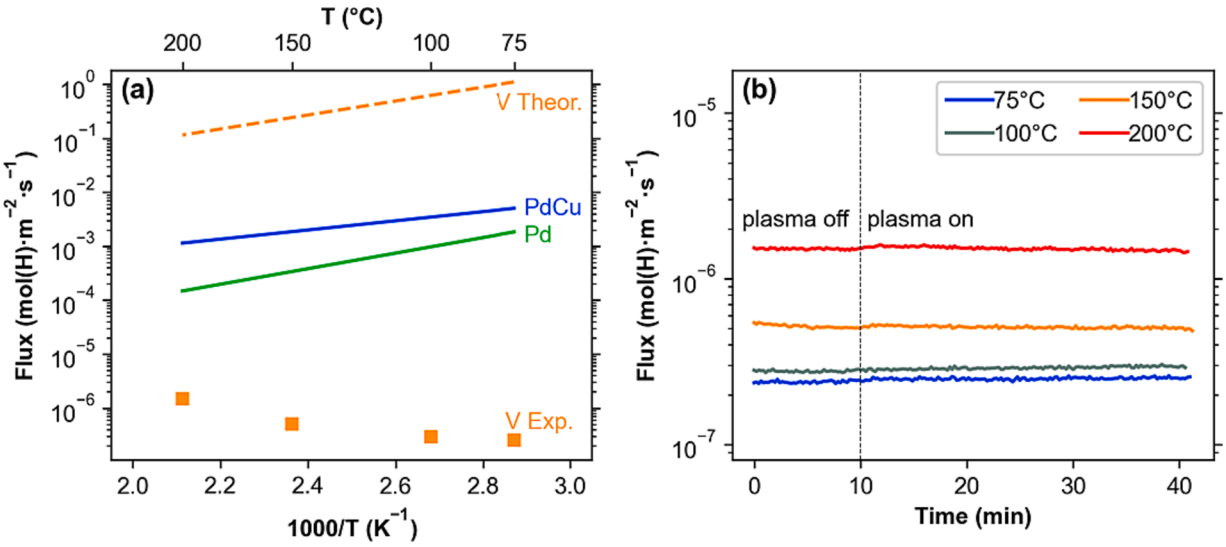

Fig. 1. (a) The flux observed under plasma permeation in pure V foil (points) and its comparison with both theoretical expectations for Sieverts' law under these conditions (dashed line) and experimental values of plasma permeation obtained with Pd and PdCu foils (solid lines) [40]; (b) transient behavior of plasma permeation in V showing that the plasma does not enhance flux.

susceptor and exposed to a 50 W radio frequency (RF) plasma for 30 min, operating at a pressure of 0.67 Pa in an argon atmosphere and a direct current (DC) bias of approximately 310 V. This is the same procedure used to obtain high superpermeation in Pd-based foils [40]. Pd layers were deposited onto the clean V surface without breaking vacuum by DC sputtering with a 45 W power applied to a cm diameter Pd target (99.95% purity, Kurt J. Lesker,). The Pd deposition rate was calibrated and fixed at 100 nm/15 min at room temperature. Pd60Cu40 (wt.%) layers were deposited by co-sputtering Pd and Cu at room temperature, where the Pd sputtering conditions were the same as above, while for the Cu part, a DC power of 57 W was applied to a 5 cm-diameter Cu target (99.99% purity, Kurt J. Lesker). The as-deposited PdCu layer was then annealed in the sputtering chamber at a base pressure of $< 5 \times 10^{-5}$ Pa at 250 °C for 2 h to ensure complete transformation of the crystal structure to the body-centered cubic (BCC) phase (See SI-Figs. 2 & 3). Crystal structures of composite membranes, both before and after plasma permeation, were analyzed through X-ray diffraction (XRD) utilizing a PANalytical 103 PW3040 X-ray diffractometer using Cu Kα radiation. To both optimize performance and improve our mechanism understanding a combination of symmetric and asymmetric composite membranes were fabricated and tested as summarized in Table 1.

2.2. Membrane evaluation

All hydrogen plasma permeation experiments performed in this study were carried out using the same setup detailed in our previous work [40]. Membranes with an effective permeation area of $A = 0.93\ cm^2$ were sealed in a Swagelok VCR fitting module which separates the feed side chamber and a permeate side chamber. We have used this identical configuration in conventional high temperature gas permeation and achieved experimental permeability's within ± 5% of theoretical values for pure Pd and PdCu foils, which reflects the uncertainty in absolute values. The membrane temperature, T_m, was actively controlled by a PID controller connected to a thermocouple and a resistive heating wire. Ultra-high purity (UHP) grade H_2 was delivered through a mass flow controller and the upstream pressure P_1 was measured by a capacitance gauge (0.1–1000 Pa). The feed side was evacuated by a turbomolecular pump with a nominal pumping speed of

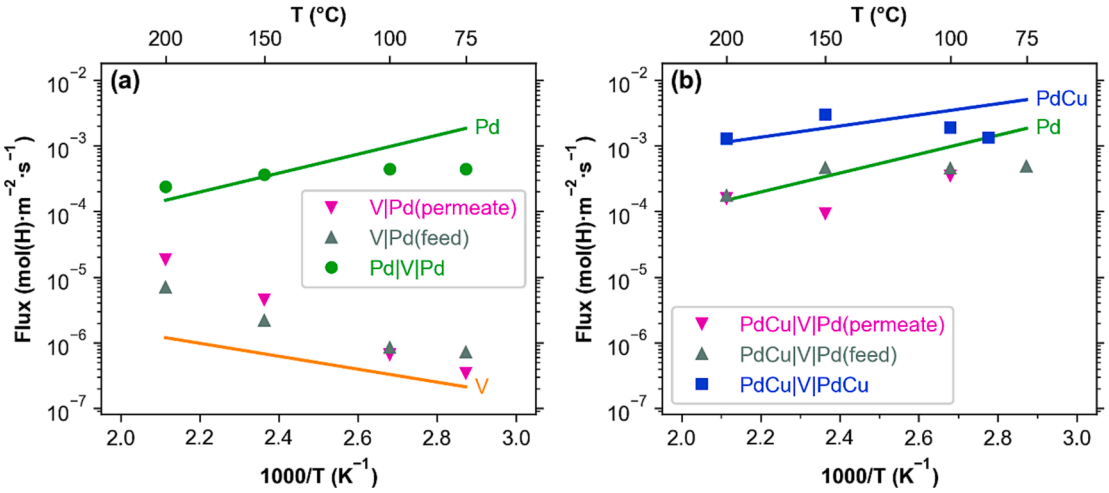

Fig. 2. Arrhenius plots showing plasma permeation through (a) symmetric and asymmetric Pd-V composite membranes and (b) symmetric and asymmetric PdCu-V composites compared with the performance of pure metal foils (lines) of V (orange), Pd (green), and PdCu (blue) under identical conditions. (For interpretation of the references to colour in this figure legend, the reader is referred to the web version of this article.)

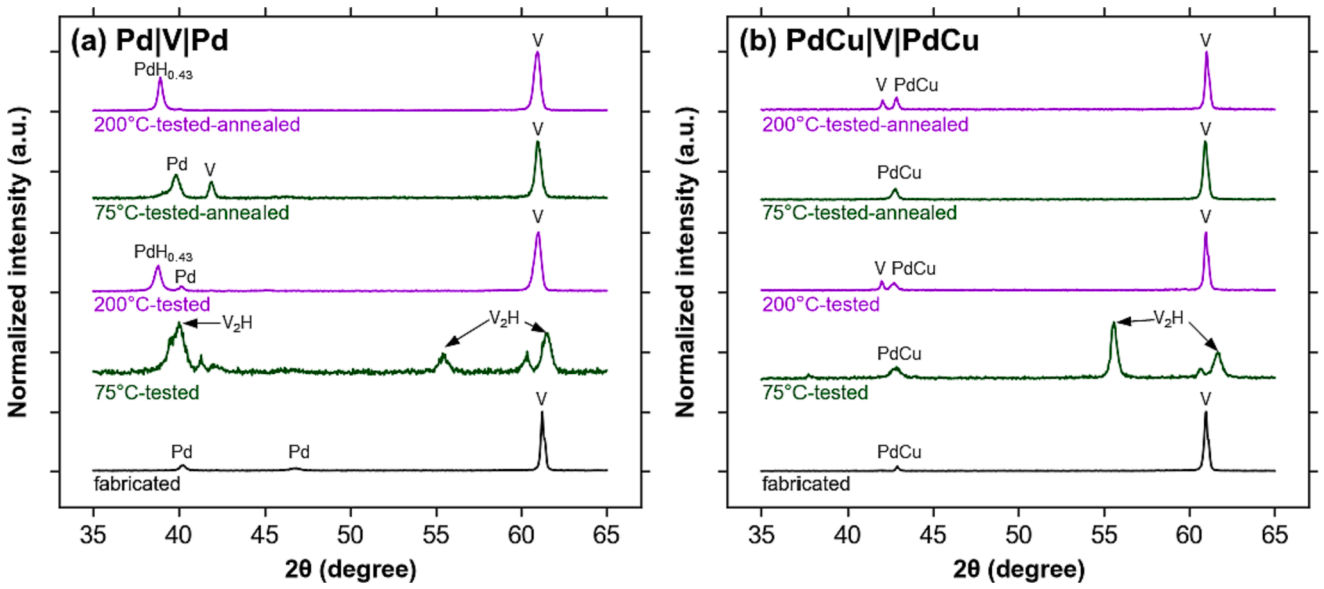

Fig. 3. XRD comparison of feed side of (a) Pd|V|Pd and (b) PdCu|V|PdCu composite membranes in the as-fabricated state (black) and after testing at 75 °C (green), 200 °C (purple), and corresponding samples after vacuum annealing. Peak references: V ICDD 00-022-1058 (42.171, 61.160); Pd ICDD 00-046-1043(40.118, 46.658); BCC-PdCu ICDD 04-015-2413(42.868); V_2H ICDD 04-007-2400(40.549, 55.487, 61.783); $PdH_{0.43}$ ICDD 00-068-0101(39.029). (For interpretation of the references to colour in this figure legend, the reader is referred to the web version of this article.)

Table 1
List of all membranes studied in the paper.

No.	Foil	Note
1	V	100 μm
2	V|Pd(feed)	Pd layer (100 nm) only on the feed side
3	V|Pd(permeate)	Pd layer (100 nm) only on the permeate side
4	Pd|V|Pd	Pd layers (100 nm) on both sides
5	PdCu|V|Pd(feed)	Pd layer (100 nm) on the feed side; PdCu (120 nm, bcc)
6	PdCu|V|Pd (permeate)	Pd layer (100 nm) on the permeate side; PdCu (120 nm, bcc)
7	PdCu|V|PdCu	PdCu (120 nm, bcc) on both sides

48 l/s for H_2 and an RF power source (13.56 MHz) coupled to a water-cooled coil outside the quartz tube was used to generate an inductively coupled plasma. In all permeation tests presented below, the plasma conditions were fixed at 100 W of RF power and $P_1 = 6.5$ Pa to ensure a constant incident flux of H atoms. The permeate side chamber was maintained at an ultra-high vacuum base condition through a second turbomolecular pump with a nominal H_2 pumping speed of 40 l/s. During permeation tests, the permeate chamber pressure, P_2, was monitored by a cold cathode vacuum sensor (10^{-9} – 10^{-2} Pa). In addition, a residual gas analyzer was used to analyze the gas composition in the permeate side chamber and to ensure no leaks by continuously monitoring the H_2O (18) and N_2 (28) signals. In a permeation test, the steady-state permeate chamber pressure P_2 was recorded and converted into the hydrogen molar flowrate n_{H_2}, and then the experimental permeation flux can be calculated by the following equation:

$$J_H = 2n_{H_2}/A \tag{2}$$

where J_H is the atom H permeation flux in mol(H)·m^{-2}·s^{-1}; A is the effective membrane permeation area. This approach is called the flux method [19] and it is based on establishing relationships between P_2 and n_{H_2} in the downstream chamber. Therefore, a meticulous calibration work was done in our previous study [40] to obtain the curve of n_{H_2} as a function of P_2 in the above experimental setup.

3. Results

3.1. Composite vanadium foil performance

Fig. 1**(a)** displays a comparison of the plasma permeation flux observed among pure V foil (orange squares), a pure Pd foil (green solid line), and a bcc-PdCu foil (blue solid line), and the theoretical gas driven flux expected based on vanadium permeability and Sieverts' law (orange dashed line) at these conditions. The Pd and PdCu flux lines are Arrhenius fits to our previous experimental data obtained under identical conditions [40]. At the small driving force of just $\Delta P = 6.5$ Pa the expected flux based on gas driven permeation is exceptionally high due to the excellent bulk permeability of vanadium. However, due to very poor surface kinetics the observed flux is 7–8 orders of magnitude lower. The kinetic limitation is further confirmed by its temperature dependency, where higher temperatures result in higher flux in the V foil while the bulk permeability declines with temperature. As shown in Fig. 1**(b),** the flux through vanadium is nominally identical before or after plasma ignition at t = 10 min, showing that there is no super-permeation under these conditions. It is generally assumed that the barrier to absorption of superthermal H is negligible. While this may be true at high temperatures where V has conventionally been tested, there appears to be a significant barrier to absorption under these low temperature conditions. **SI**-Fig. 4 presents the XRD comparison between the V membrane before and after plasma permeation test. The as-received cold rolled foils display a preferential orientation in the 200 direction, and the pattern is unchanged after testing, consistent with limited hydrogen absorption.

In contrast, a step increase in permeation is observed with Pd-based foils upon plasma ignition (see Fig. 5), and the measured flux is 3–4 orders of magnitude greater than V. For both Pd and PdCu foils the plasma permeation decreases as the temperature is elevated, consistent with absorption being the rate limiting step as discussed in our previous work [40]. While the mechanism is the same PdCu displays 3-5X higher flux than Pd which is attributed to its superior desorption kinetics.

To better understand and overcome the limitation of pure vanadium foils 100 nm of Pd was applied to V in both asymmetric and symmetric configurations. Fig. 2**(a)** illustrates the temperature-dependent behavior of hydrogen fluxes in V|Pd(permeate), V|Pd(feed), and Pd|V|Pd

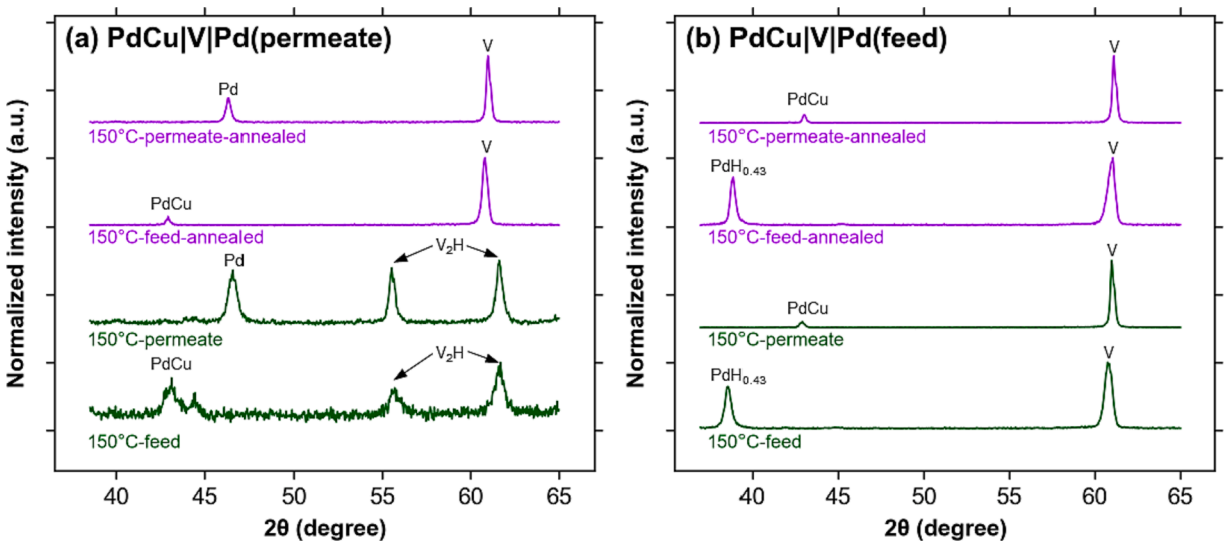

Fig. 4. XRD comparison of both sides of (a) PdCu|V|Pd(permeate) and (b) PdCu|V|Pd(feed) membranes after testing at 150 °C (green) and corresponding samples after annealing (purple). Peak references: V ICDD 00-022-1058 (42.171, 61.160); Pd ICDD 00-046-1043(40.118, 46.658); BCC-PdCu ICDD 04-015-2413(42.868); V_2H ICDD 04-007-2400 (55.487, 61.783); $PdH_{0.43}$ ICDD 00-068-0101(39.029). (For interpretation of the references to colour in this figure legend, the reader is referred to the web version of this article.)

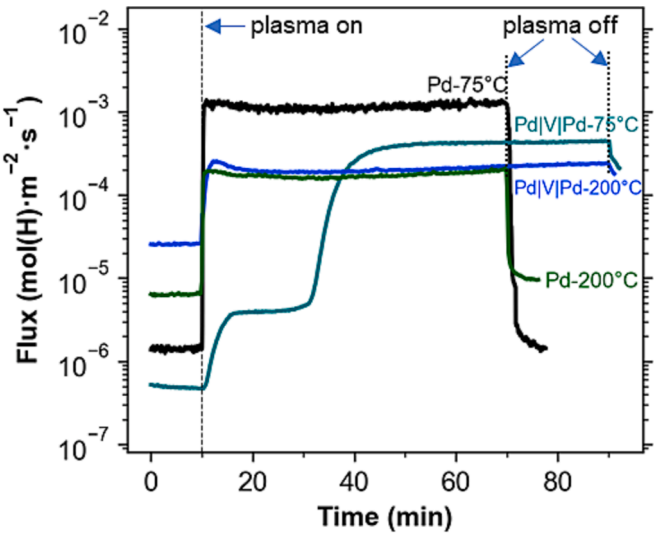

Fig. 5. Comparison of transient behavior of plasma permeation in Pd|V|Pd composite and pure Pd foil (corresponding to Fig. 2**(a)**), plasma switched on at t = 10 min in all cases and extinguished as indicated in graph.

composites are compared to Arrhenius fits of pure Pd and V foils. First, to test the hypothesis that V performance was limited by hydrogen desorption, Pd was applied to the permeate side. There was a significant increase in flux, up to an order of magnitude at T = 200 °C, but the performance remains orders of magnitude below the pure Pd foil. Likewise, when the orientation was reversed with Pd on the feed side there was a similar marginal improvement in flux. This suggests that V presents kinetic limitations to *both* molecular hydrogen desorption downstream, *and* absorption of superthermal hydrogen upstream. This was confirmed by the performance of the symmetric Pd|V|Pd membrane, which elevated performance orders of magnitude to levels comparable to the pure Pd foil. At T ≥ 150 °C the composite performance is equal to the Pd foil, showing that flux is controlled completely by the Pd layers. Hydrogen diffusion within the V foil as well as transport across the V|Pd interfaces are sufficiently fast as to not impact performance. The V foil is 4X thicker than the Pd foil (25 μm), further supporting the absence of any diffusion limitations. When the temperature is reduced to 100 °C and below the flux saturates, deviating from the pure Pd foil which continues to improve as the temperature is reduced. The reasons for this are discussed in the following section.

In our pure foil study the BCC PdCu foil outperformed Pd due to its superior surface kinetics [40]. Consistent with that finding the symmetric PdCu|V|PdCu elevated performance above Pd to the levels of the pure PdCu foil (Fig. 2**(b)**). Again, the composite performance is equal to the PdCu foil at T ≥ 150 °C, with deviations from pure foil behavior as the temperature is reduced for similar reasons with Pd as discussed below. Fig. 2**(b)** also displays the performance of an asymmetric PdCu|V|Pd composites operated in both orientations. Regardless if the Pd was placed on the feed or permeate side, the performance of these asymmetric composites was essentially reduced to that of the symmetric Pd|V|Pd composite, showing that the Pd layer is rate limiting. This shows that PdCu is superior to Pd for *both* desorption of molecular hydrogen downstream (as already understood), and absorption of superthermal hydrogen upstream. The total thickness of the sputtered layers is ~ 200 nm, meaning that these composite membranes offer Pd performance with a 99.2% reduction in Pd inventory relative to the freestanding 25 μm foils.

3.2. *Low temperature performance*

As shown in Fig. 2 the performance deviates from pure foil performance for both the Pd and PdCu composites as the temperature was reduced to 100 °C and below. This deviation from pure foil performance was correlated with the appearance of vanadium hydride (β-V_2H), as evidenced by XRD and reflected in transient performance. Fig. 3**(a)** displays the XRD evolution of the symmetric Pd|V|Pd composite membrane as a function of processing conditions. For clarity Fig. 3 displays XRD scans from the feed side of the membrane. Scans from the permeate side are included in the supplementary information (**SI-**Fig. 5), and are nominally identical with the exception of one notable feature described below. The peaks of the as-deposited sample are simply the superposition of the peaks of Pd and V. Following plasma permeation testing at 75 °C, noticeable changes occurred in the XRD pattern of the Pd|V|Pd composite. The primary V peak at 2θ = 61.16° vanished, replaced by numerous signals including those at 2θ = 55.48° and 61.78° positions, which are attributed to β-V_2H. To clarify that the new peaks are due to the formation of V hydride(s) and not other species such as possible Pd-V

alloy formation, samples were annealed under vacuum condition (<5 × 10^{-5} Pa) at 250 °C for 5 h to remove hydrogen. The subsequent XRD pattern reverted back to the as-fabricated state, with only minor changes in the intensity of characteristic peaks.

In contrast, no evidence of V hydride formation was observed on the composite membrane after testing at 200 °C. However, the original Pd peak was attenuated, and a prominent peak appeared near 2θ = 39°, which is attributed to the formation of β-$PdH_{0.43}$. This Pd hydride phase was not observed at low temperature, nor was it observed on the permeate side of the membrane at 200 °C. Its formation required both high temperature and exposure to hydrogen plasma. This peak persisted after vacuum annealing (250 °C/5h), indicating the formation of a stable compound. This is consistent with the work of Zhao et al. [56], who showed that the β-$PdH_{0.43}$ hydride phase showed no changes in its XRD pattern even after a 10-month storage in air at room temperature or after annealing for 2 h at 300 °C in an argon environment. However, the formation of Pd hydride on the feed side seems to have no effect on the permeation results (Fig. 2**a**).

Similar behavior was observed in PdCu|V|PdCu composites. Fig. 3 **(b)** compares the XRD patterns in the PdCu|V|PdCu membranes as fabricated, after testing at 75 °C (set point) and 200 °C, and corresponding samples after annealing (250 °C/5h in vacuum). Note that at a setpoint of 75 °C the sample gradually heated up to 90 °C despite no external heating during testing which was attributed to the exothermic hydrogen recombination reaction on the surface facilitated by PdCu. Again, these patterns reflect the feed side with the corresponding permeate side patterns appearing in **SI-**Fig. 6. The as-fabricated membranes exhibit a superposition of peaks from both V and BCC-PdCu. Similar to the Pd composite after plasma permeation at 75 °C, the main V peak at 2θ = 61.16° is attenuated and replaced by new peaks including those of β-V_2H. Again, vacuum annealing removed these hydride peaks and returned the sample to its as-fabricated state. For the sample tested at 200 °C, no evidence of V hydride formation was observed. There is also no evidence of a Pd-based hydride, which is consistent with the much lower hydrogen solubility in PdCu relative to Pd (**SI-**Fig. 1). After testing at 200 °C there is the appearance of a small peak at 2θ = 42.17°, which is V(1 1 0). Thus, plasma permeation at 200 °C does lead to some re-structuring of the V from its cold-rolled state.

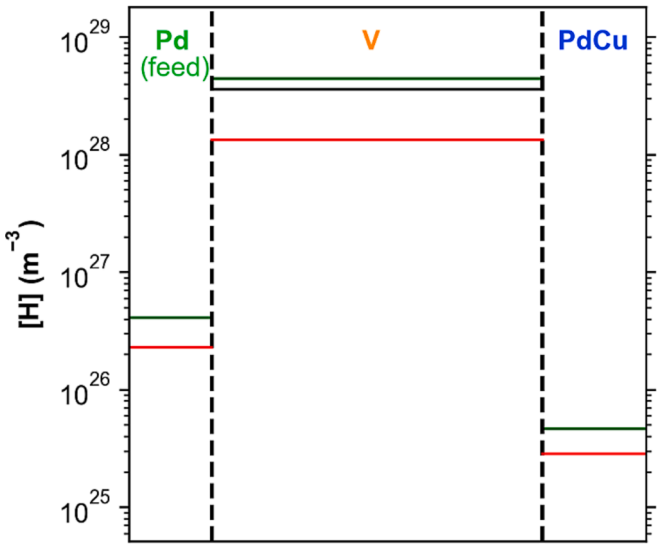

Fig. 6. Estimated [*H*] distribution throughout an asymmetric Pd(feed)|V|PdCu composite membrane at 150 °C (green) and 200 °C (red) based on **Eqs.** (1) & (3). The black line is the H density of V_2H. Note that the horizontal direction is not to scale as the V foil (100 μm) is 1000X thicker than the Pd/PdCu layers (100 nm). (For interpretation of the references to colour in this figure legend, the reader is referred to the web version of this article.)

The formation of vanadium hydride was observed in all composites whose permeance fell below its pure foil counterpart. This was also observed in asymmetric composites. For example, at T = 150 °C the PdCu|V|Pd(feed) membrane matched that of the pure Pd foil while the flux observed with the reverse orientation PdCu|V|Pd (permeate) was attenuated by a factor of ~3 (Fig. 3**(b)**). The XRD analysis (Fig. 4) of these membranes was perfectly consistent with the observations of the symmetric membranes described above. After plasma permeation at T = 150 °C the PdCu|V|Pd (permeate) showed the formation of β-V_2H, which was subsequently reduced upon annealing (Fig. 4**(a)**). In contrast, no formation of V hydride was observed in the PdCu|V|Pd(feed) membrane; instead, a stable β-$PdH_{0.43}$ compound formed on the feed side surface (Fig. 4**(b)**). At this temperature Pd cannot efficiently desorb molecular hydrogen but PdCu catalyzes the absorption of superthermal hydrogen, resulting in hydrogen accumulation in the membrane leading to hydride formation and attenuation of performance. In the reverse configuration the superior desorption kinetics of PdCu prevents hydrogen accumulation and hydride formation.

These two samples unambiguously confirm that the formation of β-V_2H is responsible for attenuation of flux from levels of the pure Pd based foils. Hydride formation was also reflected in the transient response. The transient response of a symmetric Pd|V|Pd membrane and pure Pd are compared in Fig. 5 at 75 and 200 °C. For the Pd foil a step change in flux is observed upon plasma ignition at both temperatures, with a higher steady state value obtained at T = 75 °C. At 200 °C the response of the Pd|V|Pd composite is nominally identical to the Pd foil. A much different profile is observed in the Pd|V|Pd composite at T = 75 °C. There is an increase upon plasma ignition, but the gain is attenuated and appears to saturate for ~15 min before undergoing a second increase that brings it to its steady state value, which again falls below the Pd foil at 75 °C. Our interpretation is that the initial plateau is due to the formation of the β-V_2H phase. Upon plasma ignition superthermal hydrogen rapidly enters the membrane but instead of permeating it accumulates through the formation of β-V_2H. Once this phase transformation is complete and its solubility limit is reached, hydrogen can then begin to permeate. However, it takes nearly an hour to reach a steady state and the flux is attenuated relative to the Pd foil. Very similar transients were observed in PdCu|V|PdCu composites at low temperature as well **(SI-**Fig. 7**)**.

The transient response suggests that the hydrogen diffusivity is significantly attenuated in the hydride phase or there are barriers to hydrogen transport at the β-V_2H|Pd (β-V_2H|PdCu) interfaces. Indeed, the diffusivity of H in β-V_2H is reported to be 2–3 orders of magnitude slower than in V [57]. Additionally, evidence of a transport barrier at the β-V_2H|Pd or V|Pd interface is provided by comparing the transient response upon plasma extinction. In the case of the Pd foil the response was nominally a step function, instantly returning to the pre-plasma flux levels. In contrast, the composite Pd|V|Pd membranes declined much slower at both temperatures. This shows that the V foil provides a reservoir of hydrogen that delays the transient response of these membranes, limited by the rate of hydrogen transfer from V to the Pd.

4. Discussion

The previous section clearly shows that when present the β-V_2H phase is rate limiting, which is attributed to the low H diffusivity in the β-V_2H phase, and it is expected that there are gradients across the membrane during operation. Although the foils remained intact and did not suffer catastrophic embrittlement, it is obviously desirable to operate at temperatures sufficiently high to prevent hydride formation and maximize the flux. The nominally identical behavior of symmetric composites and the Pd-based foils at 150–200 °C shows that the 100 nm layers control performance and are behaving essentially as bulk layers. Vanadium provides ample solubility and diffusivity that it is simply serves as a conduit for H to the Pd layer on the permeate side. It is presumed that superthermal absorbs in the feed layer and thermalize,

achieving a steady state concentration based on the incident H flux. Diffusion is sufficiently fast that the H distribution is constant within a given layer and the distribution through the composite structure is dictated by the relative solubility among the layers, as defined by **Eq. (3)** [51]:

$$\frac{[H]_a}{[H]_b} = \frac{S_a}{S_b} \tag{3}$$

where S is hydrogen solubility in materials a and b, respectively.

To provide further support this explanation, the [H] distribution in each layer of the PdCu|V|Pd(feed) membrane was estimated at temperatures of 150 and 200 °C using **Eqns. (1) and (3)** as follows. As in our previous study [40], the hydrogen concentration in the PdCu was calculated from **Eq. (1)** using the experimental measure of hydrogen flux (J_H)and literature values [38,39] of the desorption coefficient (k_d) to estimate the hydrogen density in the PdCu layer. The hydrogen densities in the V and Pd layers were then evaluated based on **Eq. (3)** and the relative solubilities (**SI-**Fig. 1**(c)**). Fig. 6 displays the estimated H profiles through the asymmetric membrane at steady state at T = 150 and 200 °C. For reference the H density in β-V_2H is included for comparison. Using this approach the estimated H density in the Pd layer of this asymmetric is in agreement with values expected in a bulk Pd foils at both temperatures [40]. As expected, the hydrogen density is enhanced at lower temperature, and interestingly as the temperature is reduced from 200 to 150 °C the estimated [H] density in the V foil increases beyond the β-V_2H level. This is consistent with 150 °C being the transition temperature where the β-V_2H phase starts to be detected.

Eq. (1) suggests that the flux would be maximized by combining the high solubility of V with the efficient desorption kinetics of PdCu. At a thickness of 100 nm this was not achieved, as the composite membrane performance was dictated by the bulk properties of exterior layers. Nevertheless, the potential exists that this might be achieved by reducing the thickness of the catalyst layer and this possibility that will be explored in future work. Moreover, it is expected that the composite concept demonstrated herein may be extended to develop high performance MFPs with other combinations of base metals and catalyst layers through the appropriate choice of material properties. For example, different catalyst layers could be explored whose combination of H solubility and desorption kinetics exceeds that of PdCu. Likewise, this composite membrane approach could be applied to alternative base metals. In the case of the base foil the critical material properties are hydrogen solubility and diffusivity. For example, low temperature operation could potentially be improved in the case of alloys such as V–4Cr–4Ti that have lower hydrogen solubility and thus would be resistant to hydride formation [53]. Using these principles composite MFPs could be designed for specific conditions (T, P, irradiation conditions, etc.) to achieve superior performance than what could be achieved with a single material.

An open question is the performance of these materials in the presence of contaminants that are expected to be present in a practical fusion environment. In conventional high temperature permeation Pd-based alloys have been shown to be quite robust and unaffected by up to 10,000 ppm of common impurities such as NH_3, CH_4, CO, CO_2 and N_2 [58]. Hydrocarbon pump oil is known to be detrimental, but reversible through simple oxidation/annealing treatments. How these membranes perform in the presence of impurities at lower temperature in the presence of plasma is unclear, and such studies are planned.

5. Conclusions

Herein we described the fabrication and testing of V-based composite membranes for hydrogen superpermeation at low temperature. Symmetric Pd|V|Pd and PdCu|V|PdCu membranes exhibited comparable performance to pure Pd or PdCu foils at T ≥ 150 °C, with the bulk properties of Pd-based catalyst layer serving as the rate-limiting factor. At T < 150 °C flux was reduced by a factor of 2–3 which coincided with the formation of β-V_2H. The reduced performance and poor transient response was attributed to the low H diffusivity in β-V_2H in relative to V. Annealing above 150 °C removed the hydride and restored performance. These composite membranes offer an alternative to bulk foils of Pd and its alloys for low-temperature hydrogen isotope recovery in future fusion plants employing a DIR design. Moreover, it is expected that the composite concept demonstrated herein may be extended to develop high performance MFPs with other combinations of base metals and catalyst layers through the appropriate choice of materials.

CRediT authorship contribution statement

Chao Li: Conceptualization, Investigation, Methodology, Visualization, Formal analysis, Writing – original draft. **J. Douglas Way:** Conceptualization, Supervision. **Thomas F. Fuerst:** Writing – review & editing. **Colin A. Wolden:** Project administration, Funding acquisition, Conceptualization, Supervision, Formal analysis, Writing – review & editing.

Declaration of Competing Interest

The authors declare that they have no known competing financial interests or personal relationships that could have appeared to influence the work reported in this paper.

Data availability

Data will be made available on request.

Acknowledgements

This research was supported by the U.S. Department of Energy (DOE), the Advanced Research Projects Agency Energy (ARPA-E) under contract no. DE-AR0001368. Any opinions, findings, conclusions or recommendations expressed in this publication are those of the authors and do not necessarily reflect the views of the Department of Energy or ARPA-E.

Appendix A. Supplementary data

Supplementary data to this article can be found online at https://doi.org/10.1016/j.nme.2023.101529.

References

[1] J. Tollefson, E. Gibney, Nuclear-fusion lab achieves 'ignition': what does it mean? Nature 612 (2022) 597–598, https://doi.org/10.1038/d41586-022-04440-7.
[2] Fact Sheet: Developing a Bold Vision for Commercial Fusion Energy | OSTP, The White House, 2022. https://www.whitehouse.gov/ostp/news-updates/2022/03/15/fact-sheet-developing-a-bold-vision-for-commercial-fusion-energy/ (accessed July 9, 2023).
[3] DOE Announces $46 Million for Commercial Fusion Energy Development, Energy.Gov. (n.d.). https://www.energy.gov/articles/doe-announces-46-million-commercial-fusion-energy-development (accessed July 9, 2023).
[4] Fusion Industry Association, The global fusion industry in 2022, 2023.
[5] S. Takeda, A.R. Keeley, S. Managi, How Many Years Away is Fusion Energy? A Review, J Fusion Energ. 42 (2023) 16, s10894-023-00361-z, doi: 10.1007/s10894-023-00361-z.
[6] C. Bachmann, S. Ciattaglia, F. Cismondi, G. Federici, T. Franke, C. Gliss, T. Härtl, G. Keech, R. Kembleton, F. Maviglia, M. Siccinio, Key design integration issues addressed in the EU DEMO pre-concept design phase, Fusion Eng. Des. 156 (2020), 111595, https://doi.org/10.1016/j.fusengdes.2020.111595.
[7] Powering the Future Fusion and Plasmas, 2020. https://science.osti.gov/-/media/fes/fesac/pdf/2020/202012/FESAC_Report_2020_Powering_the_Future.pdf.
[8] H. Yamada, Nuclear Fusion, in: M. Lackner, B. Sajjadi, W.-Y. Chen (Eds.), Handbook of Climate Change Mitigation and Adaptation, Springer New York, New York, NY, 2021, pp. 1–45. Doi: 10.1007/978-1-4614-6431-0_31-3.
[9] M. Abdou, M. Riva, A. Ying, C. Day, A. Loarte, L.R. Baylor, P. Humrickhouse, T. F. Fuerst, S. Cho, Physics and technology considerations for the deuterium–tritium fuel cycle and conditions for tritium fuel self sufficiency, Nucl. Fusion. 61 (2021), 013001, https://doi.org/10.1088/1741-4326/abbf35.

[10] C. Day, T. Giegerich, Development of Advanced Exhaust Pumping Technology for a DT Fusion Power Plant, IEEE Trans. Plasma Sci. 42 (2014) 1058–1071, https://doi.org/10.1109/TPS.2014.2307435.

[11] B. Bornschein, M. Glugla, K. Günther, R. Lässer, T.L. Le, K.H. Simon, S. Welte, Tritium tests with a technical PERMCAT for final clean-up of ITER exhaust gases, Fusion Eng. Des. 69 (2003) 51–56, https://doi.org/10.1016/S0920-3796(03)00234-5.

[12] C. Day, T. Giegerich, The Direct Internal Recycling concept to simplify the fuel cycle of a fusion power plant, Fusion Eng. Des. 88 (2013) 616–620, https://doi.org/10.1016/j.fusengdes.2013.05.026.

[13] T. Haertl, C. Day, T. Giegerich, S. Hanke, V. Hauer, Y. Kathage, J. Lilburne, W. Morris, S. Tosti, Design and feasibility of a pumping concept based on tritium direct recycling, Fusion Eng. Des. 174 (2022), 112969, https://doi.org/10.1016/j.fusengdes.2021.112969.

[14] B.J. Peters, S. Hanke, C. Day, Metal Foil Pump performance aspects in view of the implementation of Direct Internal Recycling for future fusion fuel cycles, Fusion Eng. Des. 136 (2018) 1467–1471, https://doi.org/10.1016/j.fusengdes.2018.05.036.

[15] S. Hanke, C. Day, T. Giegerich, J. Igitkhanov, Y. Kathage, X. Luo, S. Varoutis, A. Vazquez Cortes, T. Härtl, A. Busniuk, A. Livshits, S. Merli, A. Schulz, M. Walker, K. Baumgärtner, J. Hofmann, Progress of the R&D programme to develop a metal foil pump for DEMO, Fusion Eng. Des. 161 (2020), 111890, https://doi.org/10.1016/j.fusengdes.2020.111890.

[16] A.I. Livishits, M.E. Notkin, A.A. Samartsev, A.O. Busnyuk, A.Y. Doroshin, V. I. Pistunovich, Superpermeability to fast and thermal hydrogen particles: applications to the pumping and recycling of hydrogen isotopes, J. Nucl. Mater. 196–198 (1992) 159–163, https://doi.org/10.1016/S0022-3115(06)80023-1.

[17] Y. Nakamura, S. Sengoku, Y. Nakahara, N. Suzuki, H. Suzuki, N. Ohyabu, A. Busnyuk, M. Notkin, A. Livshits, Deuterium pumping experiment with superpermeable Nb membrane in JFT-2M tokamak, J. Nucl. Mater. 278 (2000) 312–319, https://doi.org/10.1016/S0022-3115(99)00243-3.

[18] T. Giegerich, C. Day, C. Gliss, X. Luo, H. Strobel, A. Wilde, S. Jimenez, Preliminary configuration of the torus vacuum pumping system installed in the DEMO lower port, Fusion Eng. Des. 146 (2019) 2180–2183, https://doi.org/10.1016/j.fusengdes.2019.03.147.

[19] B.J. Peters, Development of a Hydrogen-Selective Vacuum Pump on the Basis of Superpermeation = Entwicklung einer auf Superpermeation basierenden, wasserstoffselektiven Vakuumpumpe, PhD Thesis, Karlsruher Institut für Technologie (KIT) (2020), https://doi.org/10.5445/IR/1000122305.

[20] A.I. Livshitz, M.E. Notkin, Y. Pustovoit, A.A. Samartsev, Superpermeability of solid membranes and gas evacuation Part II Permeation of hydrogen through a palladium membrane under different gas and membrane boundary conditions, Vacuum 29 (1979) 113–124, https://doi.org/10.1016/S0042-207X(79)80451-0.

[21] F. Waelbroeck, I. Ali-Khan, K.J. Dietz, P. Wienhold, Hydrogen solubilisation into and permeation through wall materials, J. Nucl. Mater. 85–86 (1979) 345–349, https://doi.org/10.1016/0022-3115(79)90514-2.

[22] M.A. Pick, K. Sonnenberg, A model for atomic hydrogen-metal interactions — application to recycling, recombination and permeation, J. Nucl. Mater. 131 (1985) 208–220, https://doi.org/10.1016/0022-3115(85)90459-3.

[23] A.I. Livshits, M.E. Notkin, A.A. Samartsev, Physico-chemical origin of superpermeability — Large-scale effects of surface chemistry on “hot” hydrogen permeation and absorption in metals, J. Nucl. Mater. 170 (1990) 79–94, https://doi.org/10.1016/0022-3115(90)90329-L.

[24] A.I. Livshits, M.E. Notkin, V.I. Pistunovich, M. Bacal, A.O. Busnyuk, Superpermeability: Critical points for applications in fusion, J. Nucl. Mater. 220–222 (1995) 259–263, https://doi.org/10.1016/0022-3115(94)00424-2.

[25] A.I. Livshits, M.E. Notkin, A.A. Samartsev, M.N. Solovyov, Interactions of low energy hydrogen ions with niobium: effects of non-metallic overlayers on reemission, retention and permeation, J. Nucl. Mater. 233–237 (1996) 1113–1117, https://doi.org/10.1016/S0022-3115(96)00084-0.

[26] A. Livshits, N. Ohyabu, M. Notkin, V. Alimov, H. Suzuki, A. Samartsev, M. Solovyov, I. Grigoriadi, A. Glebovsky, A. Busnyuk, A. Doroshin, K. Komatsu, Applications of superpermeable membranes in fusion: The flux density problem and experimental progress, J. Nucl. Mater. 241–243 (1997) 1203–1209, https://doi.org/10.1016/S0022-3115(97)80221-8.

[27] K. Ohkoshi, V. Alimov, K. Yamaguchi, M. Yamawaki, A.I. Livshits, The ion- and atom-driven transport of deuterium in Nb under the influence of surface impurities, J. Nucl. Mater. 5 (1999).

[28] Y. Nakamura, A. Busnyuk, H. Suzuki, Y. Nakahara, N. Ohyabu, A. Livshits, Nb interaction with hydrogen plasma, J. Appl. Phys. 89 (2001) 760–766, https://doi.org/10.1063/1.1331075.

[29] A. Busnyuk, Y. Nakamura, Y. Nakahara, H. Suzuki, N. Ohyabu, A. Livshits, Membrane bias effects on plasma-driven permeation of hydrogen through niobium membrane, J. Nucl. Mater. 4 (2001).

[30] H. Hackfort, K. Bösche, F. Waelbroeck, J. Winter, P. Wienhold, Hydrogen pumping and compression by superpermeation through iron, J. Nucl. Mater. 144 (1987) 10–16, https://doi.org/10.1016/0022-3115(87)90273-X.

[31] T. Nagasaki, R. Yamada, M. Saidoh, H. Katsuta, Simultaneous ion and gas driven permeation of deuterium through nickel, J. Nucl. Mater. 151 (1988) 189–201, https://doi.org/10.1016/0022-3115(88)90071-2.

[32] T. Nagasaki, R. Yamada, H. Ohno, Permeation of deuterium implanted into copper, J. Nucl. Mater. 179–181 (1991) 335–338, https://doi.org/10.1016/0022-3115(91)90094-N.

[33] P.L. Andrew, A.A. Haasz, Models for hydrogen permeation in metals, J. Appl. Phys. 72 (1992) 2749–2757, https://doi.org/10.1063/1.351526.

[34] B. Dean, A.A. Haasz, P.C. Stangeby, Sticking coefficient of molecular and atomic hydrogen on palladium, J. Vac. Sci. Technol. A 5 (1987) 2332–2335, https://doi.org/10.1116/1.574446.

[35] A.B. Antoniazzi, A.A. Haasz, P.C. Stangeby, The effect of adsorbed carbon and sulphur on hydrogen permeation through palladium, J. Nucl. Mater. 162–164 (1989) 1065–1070, https://doi.org/10.1016/0022-3115(89)90410-8.

[36] A.B. Antoniazzi, A.A. Haasz, P.C. Stangeby, The effect of the surface state on the permeation of hydrogen through palladium, J. Vac. Sci. Technol. A 5 (1987) 2325–2331, https://doi.org/10.1116/1.574445.

[37] A.B. Antoniazzi, A.A. Haasz, O. Auciello, P.C. Stangeby, Atomic, ionic and molecular hydrogen permeation facility with in situ Auger surface analysis, J. Nucl. Mater. 128–129 (1984) 670–675, https://doi.org/10.1016/0022-3115(84)90432-X.

[38] I. Takagi, K. Moritani, H. Moriyama, Asymmetric surface recombination of hydrogen on palladium exposed to plasma, J. Nucl. Mater. 313–316 (2003) 102–106, https://doi.org/10.1016/S0022-3115(02)01370-3.

[39] M. Onaka, I. Takagi, T. Kobayashi, T. Sasaki, A. Kuzmin, H. Zushi, Characteristic of a pdCu membrane as atomic hydrogen probe for QUEST, Nuclear Materi. Energy 9 (2016) 104–108, https://doi.org/10.1016/j.nme.2016.09.001.

[40] C. Li, A.J. Job, T.F. Fuerst, M. Shimada, J.D. Way, C.A. Wolden, Low temperature hydrogen plasma permeation in palladium and its alloys for fuel recycling in fusion systems, J. Nucl. Mater. 582 (2023), 154484, https://doi.org/10.1016/j.jnucmat.2023.154484.

[41] Y. Hatano, A. Livshits, A. Busnyuk, M. Nomura, K. Hasizume, M. Sugisaki, Y. Nakamura, N. Ohyabu, K. Watanabe, Kinetics of Dissociative Absorption of Hydrogen through Nb Surface Covered by Oxygen, Physica Scripta. (2004) 14, https://doi.org/10.1238/Physica.Topical.108a00014.

[42] A.I. Livshits, M.E. Notkin, N. Ohyabu, Y. Nakamura, I.P. Grigoriadi, A. A. Samartsev, Hydrogen Release Through Metallic Surface: The Role of Sputtering and of the Impurity Dynamics, Phys. Scripta (2004) 23, https://doi.org/10.1238/Physica.Topical.108a00023.

[43] Y. Hatano, A. Livshits, Y. Nakamura, A. Busnyuk, V. Alimov, C. Hiromi, N. Ohyabu, K. Watanabe, Influence of oxygen and carbon on performance of superpermeable membranes, Fusion Eng. Des. 81 (2006) 771–776, https://doi.org/10.1016/j.fusengdes.2005.06.368.

[44] S. Tominaga, A. Busnyuk, T. Matsushima, K. Yamaguchi, F. Ono, T. Terai, M. Yamawaki, Study of Carbon Deposition Effect on Hydrogen Permeation Through Palladium Membrane, Fusion Sci. Technol. 41 (2002) 919–923, https://doi.org/10.13182/FST02-A22719.

[45] P.L. Andrew, A.A. Haasz, Effect of surface impurities on the permeation of hydrogen through iron, J. Vac. Sci. Technol. A 8 (1990) 1807–1813, https://doi.org/10.1116/1.576807.

[46] A. Livshits, N. Ohyabu, M. Bacal, Y. Nakamura, A. Busnyuk, M. Notkin, V. Alimov, A. Samartsev, H. Suzuki, F. Sube, Fuel recycling and edge plasma control with membrane techniques: plasma–membrane simulation experiments, J. Nucl. Mater. 266–269 (1999) 1267–1272, https://doi.org/10.1016/S0022-3115(98)00693-X.

[47] A.I. Livshits, F. Sube, M.N. Solovyev, M.E. Notkin, M. Bacal, Plasma driven superpermeation of hydrogen through group Va metals, J. Appl. Phys. 84 (1998) 2558–2564, https://doi.org/10.1063/1.368418.

[48] W.T. Shmayda, F. Waelbroeck, J. Winter, P. Wienhold, T. Banno, N.P. Kherani, Tritium Pumping Based on Asymmetric Permeation, Fusion Technol. 8 (1985) 2285–2289, https://doi.org/10.13182/FST85-A24621.

[49] P.L. Andrew, A.A. Haasz, Hydrogen permeation through copper-coated palladium, J. Appl. Phys. 70 (1991) 3600–3604, https://doi.org/10.1063/1.349256.

[50] P.L. Andrew, A.A. Haasz, Effect of thin copper and palladium films on hydrogen permeation through iron, J. Less Common Metals 172–174 (1991) 732–739, https://doi.org/10.1016/0022-5088(91)90197-C.

[51] Y. Xu, Y. Hirooka, L.M. Luo, Y.C. Wu, Deuterium concentration depth profiling in sputter-deposited tungsten coated F82H using secondary ion mass spectrometry, Nucl. Mater. Energy 21 (2019), 100708, https://doi.org/10.1016/j.nme.2019.100708.

[52] S. Fetter, E.T. Cheng, F.M. Mann, Long-term radioactive waste from fusion reactors: Part II, Fusion Eng. Des. 13 (1990) 239–246, https://doi.org/10.1016/0920-3796(90)90104-E.

[53] D.I. Cherkez, A.V. Spitsyn, A.V. Golubeva, V.M. Chernov, Deuterium permeation through the low-activated V–4Cr–4Ti alloy under plasma irradiation, Nucl. Mater. Energy 23 (2020), 100756, https://doi.org/10.1016/j.nme.2020.100756.

[54] D.A. Cooney, J.D. Way, C.A. Wolden, A comparison of the performance and stability of Pd/BCC metal composite membranes for hydrogen purification, Int. J. Hydrogen Energy 39 (2014) 19009–19017, https://doi.org/10.1016/j.ijhydene.2014.09.094.

[55] M.D. Dolan, D.M. Viano, M.J. Langley, K.E. Lamb, Tubular vanadium membranes for hydrogen purification, J. Membr. Sci. 549 (2018) 306–311, https://doi.org/10.1016/j.memsci.2017.12.031.

[56] Z. Zhao, X. Huang, M. Li, G. Wang, C. Lee, E. Zhu, X. Duan, Y. Huang, Synthesis of Stable Shape-Controlled Catalytically Active β-Palladium Hydride, J. Am. Chem. Soc. 137 (2015) 15672–15675, https://doi.org/10.1021/jacs.5b11543.

[57] D. Richter, S. Mahling-Ennaoui, R. Hempelmann, Hydrogen Diffusion in a One Domain β -V $_2$ H Single Crystal*, Z. Phys. Chem. 164 (1989) 907–920, https://doi.org/10.1524/zpch.1989.164.Part_1.0907.

[58] H. Yoshida, S. Konishi, Y. Naruse, Effects of impurities on hydrogen permeability through palladium alloy membranes at comparatively high pressures and temperatures, J. Less Common Metals 89 (1983) 429–436, https://doi.org/10.1016/0022-5088(83)90353-3.